

Received 1 September 2022, accepted 9 September 2022, date of publication 12 September 2022,
date of current version 16 September 2022.

Digital Object Identifier 10.1109/ACCESS.2022.3206375

RESEARCH ARTICLE

ECMS: Energy-Efficient Collaborative Multi-UAV Surveillance System for Inaccessible Regions

CHETNA SINGHAL^{1,2}, (Senior Member, IEEE), AND SUBHRAJIT BARICK¹

¹Department of Electronics and Electrical Communication Engineering, Indian Institute of Technology Kharagpur, Kharagpur, West Bengal 721302, India

²Department of Computer Science, RISE Research Institutes of Sweden AB, Kista, 164 40 Stockholm, Sweden

Corresponding author: Chetna Singhal (chetna.iitd@gmail.com)

This work was supported by the Indian Department of Science and Technology under Grant DST/INSPIRE/04/2015/000793.

ABSTRACT The evolution and popular adaptation of drone technology in diverse applications has necessitated advancement of UAV communication framework. UAVs inherently support features like mobility, flexibility, adaptive altitude, which make them a preferable option for dynamic surveillance of remote locations. Multiple UAVs can cooperatively work to accomplish surveillance missions more efficiently. However, the intermittent network connectivity and the limited onboard energy storage impose a great challenge on UAV-assisted remote surveillance. This paper presents an Energy-efficient Collaborative Multi-UAV Surveillance (ECMS) system for surveillance of inaccessible regions. The system employs an optimal Multi-UAV Collaborative Monocular Vision (MCMV) topology to facilitate the surveillance with zero blind spot using minimum number of drones. We also propose an application-aware Multi-Path Weighted Load-balancing (MWL) routing protocol for handling congestion by distributing traffic among all available resources in UAV network and adaptively selecting the of source datarate (i.e. switching video resolution). The simulation results demonstrate that the proposed surveillance system achieves coverage with lesser number of UAVs compared to the existing systems. It also achieves higher throughput, higher packet-delivery ratio, higher residual energy of UAVs, and lower end-to-end delay.


INDEX TERMS Unmanned aerial vehicle, remote surveillance, UAV network topology, multi-path routing, load balancing.

I. INTRODUCTION

With the advancement of drone technology, unmanned aerial vehicles (UAVs) have extended into new application domains, such as real-time video surveillance [1], [2], [3], search and rescue operations [4], [5], [6], [7], reconnaissance and combat operations [5], [8]. Equipped with modern on-board navigation systems, the UAVs can facilitate surveillance in tough situations in an autonomous manner. The aerial surveillance has several advantages over traditional monitoring systems: (1) it minimizes the need for field agents, (2) it limits the hazards to the persons involved, (3) it lowers the operation cost, and (4) it enhances system efficiency. However, a single UAV may not be sufficient to provide long-term and reliable surveillance due to its resource constraints. Therefore, multiple UAVs are used which form a

coordinated network to conduct an effective surveillance [9], [10]. When compared to a single-UAV system, a multi-UAV network (UAV-Net) has several advantages, including lower cost due to the use of multiple small UAVs rather than a single large powerful UAV, higher reliability in case of a failure, a larger coverage area, and more robustness due to information sharing and data fusion. However, designing such multi-UAV network for monitoring of hard-to-reach places requires an intensive investigations and is still an ongoing research challenge.

In multi-UAV surveillance, one of the challenges is to conduct surveillance with minimum number of UAVs. Therefore, it is important to develop an optimal topology for the UAV network in order to meet the goal without any blind spots. Besides this, communication among UAVs for cooperation is also critical. In addition, the energy consumption in communication is important for sustaining UAV-based surveillance as it affects the UAV-Net lifetime. The UAVs consume certain

The associate editor coordinating the review of this manuscript and approving it for publication was Guillermo Valencia-Palomo .

amount of power while streaming surveillance information to the ground control station (GCS). Since, the UAVs have limited on-board energy, lack of energy consumption management may cause certain UAVs to run out of power before others, causing the mission to fail in the middle. Therefore, developing an effective routing mechanism that can reduce the energy consumption by regulating congestion in the network is crucial to extending the network lifetime.

In this manuscript, we propose an energy-efficient Collaborative Multi-UAV Surveillance (ECMS) system that provides surveillance and communication support in inaccessible regions. The overview of the functional blocks of the proposed ECMS system, for zero blindspot surveillance in inaccessible region, are shown in Fig. 1. We first propose an optimal quality-of-service (QoS)-aware topology for UAV network, Multi-UAV Collaborative Monocular Vision (MCMV), which ensures a minimum number of UAVs cover the entire inaccessible region without any blind spots. The topology is determined by using the focal parameters of the on-board camera setup. The position of UAVs are optimally chosen to maintain the distance between the UAVs and between the UAVs and ground targets to achieve acceptable packet loss and Quality-of-Experience (QoE) for video streaming. Finally, we propose an efficient Multi-path Weighted Load balancing (MWL) routing mechanism that handles congestion in the UAV network by dynamically distributing the traffic among multiple paths and selecting the source data (and packet) rate. Hence, MWL is an application-aware multipath routing protocol that performs source adaptive congestion control.

The key contributions of this paper are listed below:

- i) We propose an ECMS system to perform surveillance in remote inaccessible area A. Therein, we develop an optimal MCMV topology to decide the minimum number of UAVs, at optimal flying height λ^* , required to conduct surveillance without any blind spot.
- ii) We also propose an efficient application-aware MWL routing strategy that reduces the end-to-end delay as well as the energy consumption, and improves the throughput along with the energy efficiency in UAV-Net based surveillance system by regulating congestion in the network.
- iii) We perform in-depth simulations to evaluate the ECMS system with respect to (w.r.t) its topology and routing method. The simulation results show that the proposed MCMV topology and the MWL routing perform efficiently when compared to alternative schemes.

The remaining paper is structured as follows. Section II reviews the related works on the subject. Section III gives an overview of ECMS system model. Section IV discusses the MCMV optimal network topology solution for remote surveillance. Section V highlights the MWL routing protocol for efficient transmission of surveillance video from UAVs to Ground Control station. Section VI presents the test-bed details and performance analysis of the ECMS system and Section VII concludes the paper.

II. RELATED WORKS

Over the past few years, a significant amount of research has been done on the UAV network for surveillance applications. In [11], the authors propose a methodology for video surveillance over 4G LTE network. The system makes use of a multi-UAV network that performs video surveillance in the area of interest by using the existing communication infrastructure. [6] develops a Wi-Fi-based emergency network to conduct on-site surveillance and transmit the information to the relief center for better rescue planning. Here, the coverage is provided by creating a Wi-Fi zone over the area of interest. In [12], the coverage issue of UAV-based surveillance in a complex urban environment is addressed. The ideal number of view points in the air to completely cover the target surface is determined by using a polynomial-time greedy set cover approach. All of the network models that have been discussed so far require the communication infrastructure, thus cannot be applied to monitor remote areas that lack communication infrastructure and are completely inaccessible. Therefore, in this work, we mainly focus on developing a network topology that can support the communication and surveillance over inaccessible region.

There have been a number of solutions to determine the UAV network topology to ensure coverage and connectivity in remote location. [13] provides a mathematical model to find the optimal UAV position for maximum coverage. The authors consider the average path loss between the UAV and the ground user as a performance parameter and determine

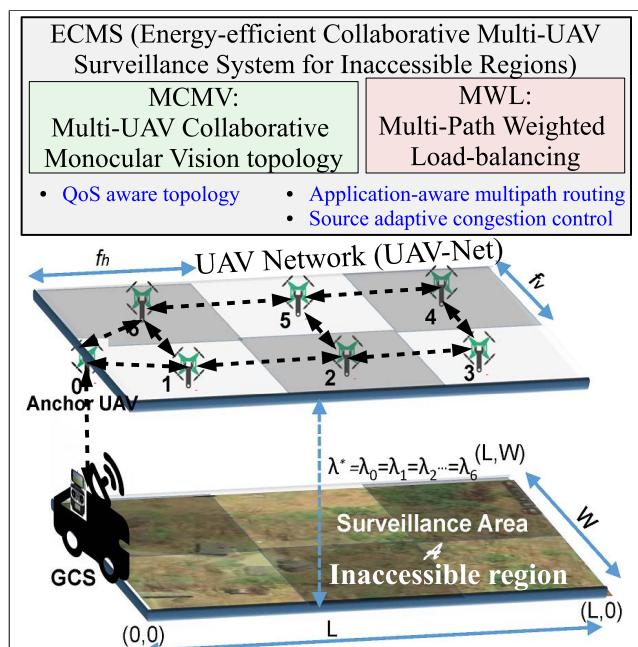


FIGURE 1. Functional components of ECMS system for zero blindspot surveillance in inaccessible region.

the optimum operational height for maximum coverage. [14] proposes a mathematical model to find the inter UAV distances in a multi-UAV network to maximize the coverage. In [15], the authors consider a network topology for monitoring a post-disaster scenario. This gives a mathematical model to decide the optimal UAV positions for providing coverage with minimum transmitting power. A topology construction algorithm based on the particle swarm optimization (PSO) is discussed in [16]. The majority of the topology development strategies that have been described so far emphasize on maximizing the coverage. However, in our work, we have developed a network topology that enables to achieve the coverage with minimum number of UAVs.

It has been shown in [17] that determining the minimum number of drones for guaranteed coverage of a target area is NP-complete. [18] propose a methodology to decide the network topology to conduct surveillance with minimum number of UAVs. The authors consider a static UAV setup and decide the optimal UAV positions based on the camera specifications in order to cover the target region with least number of UAVs possible. To further reduce the number of UAVs needed, the authors in [19] propose a movable camera setup. A minimum number of UAVs for constrained coverage (CC) network deployment with a circular (on ground) sensing area is obtained in [20]. All of these UAV minimization techniques work under the premise that the UAVs are fixed in the intended location. However, in reality, this is not true. The UAVs are typically moving objects. As a result, a small deviation from the ideal position may result in a ground coverage hole. Therefore, in our research, we design an optimal topology to perform surveillance with no blind spots while using the minimum number of UAVs.

Drone energy consumption model depends on the drone weight, payload, flying speed, and distance covered. The total energy consumption rate consists of the avionic communication and flying operation separately [21]. For example, the avionics power is approximately 100 J/s (according to [22]) and this is equivalent to the power required by a small drone to fly less than 100 m distance at a constant altitude and less than 10 m/s airspeed [21]. The steady flight power consumption model consists of power for lift, power to overcome drag, and ascending/descending power. In literature, we find drone systems can use more than one onboard power supply for a more reliable operation [23], [24].

Wireless transmission of large volumes of data is energy consuming and can deplete the on-board energy of UAVs very quickly [25]. Higher resolution video is of larger data size and requires more network bandwidth for transmission [26]. Streaming high bitrate (high resolution) video leads to increased energy consumption in transmission [27]. Camera node generate high volumes of data and consume more energy in acquiring and transmitting video [28]. UAV network lifetime is critical to avoid disruption in the overall network [29]. Hence, in this paper we focus on energy-efficient communication of the surveillance video captured from UAV-onboard camera to the GCS in an

effective and application-aware manner. We have specifically devised an the energy efficient scheme focused on the surveillance application related communication only.

In surveillance, routing is crucial since it has a direct impact on the network's energy usage. Establishing routing paths with UAVs having higher residual energy level can guarantee a high level of communication stability [25], [29]. [30] proposes an efficient topology-based routing mechanism for faster delivery of messages to the destination. The authors choose the best next-hop UAV based on the UAVs' present locations and trajectory information. [31] illustrates that the power consumption of UAV during data transmission is proportional to the size of the transmitted data; thus, the smaller the size of transmitted data, the smaller the energy consumption. [32] develops an efficient load balancing technique for reducing network congestion in wireless LAN by using persistence weighted round-robin algorithm. In [33], the authors provide a load balancing algorithm for UAV-assisted wireless networks using SDN.

Multi-path routing in Mobile Ad-hoc Networks (MANET) and Flying Ad-hoc Networks (FANET) facilitate selection from multiple paths between source and destination node [7], [34], [35], [36]. Routing protocols for FANETs [37], [38] can be topology-based, position-based, hierarchical, deterministic, or stochastic with load balancing to provide improved quality-of-service, i.e., QoS (e.g., end-to-end delay) [36]. Multi-Path variant of Dynamic source Routing with load balancing (LMP-DSR [34]) selects a path from the route cache (maintained through Route Discovery). Ad Hoc On-Demand Distance Vector-Multipath (AODVM) routing based on link parameter information can ensure higher video quality and adaptive transmission delay [35] in UAV-Net.

Stochastic centralized Multipath UAV Routing protocol for FANETs (SMURF) computes the most reliable route [39] for transmission. Enhanced Optimized Link-State Routing protocol for FANETs (OLSRF) prevents communication interruptions due to rapid topology changes [40]. Robust multi-path communication (RMPC) in UAV systems can control network congestion by dynamically selecting the best performing path from multiple wireless multihop paths [41]. Multipath TCP (MTCP) can provide stable traffic flow control and coordination of drones [42]. Stochastic packet forwarding algorithm (SPA) [43], [44] selects the forwarding drone based on network metrics and provides efficient data transmission with improved throughput in FANETs. Success Ratio-based Routing (SRR) is a light-weight protocol for dynamic opportunistic networks that improves the packet delivery ratio [45].

In our paper, we propose an application-aware Multi-path Weighted Load balancing (MWL) routing protocol that is light-weight and achieves congestion control in the network. The routing algorithm distributes the load (video surveillance data packets) over multiple node disjoint paths based on the existing traffic in the path. We have summarised the comparison of MWL with other state-of-the-art routing protocols in terms of distinct features in Table 1. The

TABLE 1. Feature comparison between routing protocols.

Feature	Routing Protocol								
	LMP-DSR	AODVM	SMURF	OLSRF	RMPC	MTCP	SPA	SRR	MWL
Application-aware	No	No	Yes	No	No	No	No	No	Yes
Load balancing	Yes	Yes	Yes	No	No	No	Yes	No	Yes
Link existence based	No	No	Yes	Yes	Yes	No	Yes	No	Yes
Multipath	Yes	Yes	Yes	No	Yes	Yes	Yes	No	Yes
Light-weight	No	No	No	Yes	No	No	Yes	Yes	Yes
Multi-path delivery	No	No	Yes	No	No	Yes	No	No	Yes
QoS aware topology	No	No	No	No	No	No	No	No	Yes
Congestion-control	No	No	No	No	Yes	Yes	No	Yes	Yes

TABLE 2. Notations and significance of symbols.

Symbol	Significance
\mathbf{A}	Surveillance area
f_h	Horizontal field of view (FOV)
f_v	Vertical FOV
λ	UAV flying height
θ_v	Verticle angle of view (AOV)
θ_h	Horizontal AOV
$\mathcal{C}(\lambda)$	UAV coverage area at λ
S_h	Horizontal camera sensor dimension
S_v	Vertical camera sensor dimension
F_l	Camera focal length
$Q(\lambda)$	QoS at λ
\mathcal{L}	Packet loss ratio
N	Number of UAVs
\mathcal{N}	Set of UAVs in UAV-Net
$\chi_{i,j}$	Coverage overlapping between UAVs i and j
$\mathbf{A}_{i,j}$	Overlap area (on ground) for UAVs i and j
μ	Packet loss exponent
λ_{th}, λ^*	Operational threshold height
X, Y	x-y coordinate $(x_i, y_i, \forall i \in \mathcal{N})$ vector of UAVs
α	overlapping percentage on the ground
Δh	Horizontal overlapping of UAV
Δv	Vertical overlapping of UAV
K, L	Number of rows, columns in UAV grid
P_i	Indicator that i is inner or edge node
\mathcal{M}	Set of M links
\mathcal{W}	Set link weights w_k
$\sigma_{j,k}^i$	Association of source node i with link k
$A = \{\sigma_{j,k}^i\}$	Association matrix $i \in \mathcal{N}, j \in \{1, 2, 3\}, k \in \mathcal{M}$
W_j^i	Path weight, node disjoint path j , source node i
r_j^i	Traffic ratio corresponding to path j
$W_{j,inc}^i$	Increase in weight of path j of source node i
D_j^i	Data traffic distribution on path j , source node i
T	Highest data rate supported by each link

advantage of optimal topology (MCMV) is that it is QoS aware by selecting inter-node distance that limits the packet loss ratio. Furthermore, the weighted load balance along the simultaneous multiple paths for packet delivery is link existence based and application (surveillance video transmission) aware.

We have summarized the major notations used in the rest of the paper in Table 2.

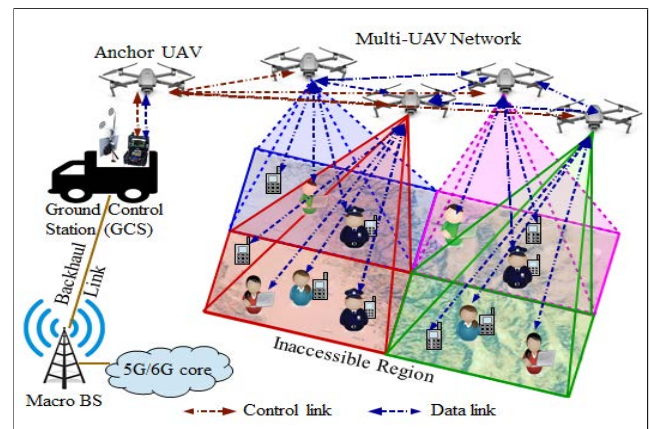


FIGURE 2. ECMS system for surveillance and communication support in inaccessible region.

III. ECMS SYSTEM MODEL

The ECMS system consists of three major components: the UAV-Net, the Anchor UAV (AU), and the GCS, as depicted in Fig. 2. The UAV-Net is a cooperative multi-UAV network consisting of N identical UAVs that performs the surveillance operation. Let $\mathcal{N} = \{1, 2, \dots, N\}$ represent the set of UAVs present in the UAV-Net. The UAVs in the UAV-Net hover at a predetermined altitude over the mission area, record the surveillance video, and then transmit it to the GCS over Wi-Fi for further processing. The AU serves as a relay, connecting the UAV-Net to the GCS. The system may include either one AU or a chain of AUs depending on the distance between the mission area and GCS. The GCS is the on-ground control unit for managing the surveillance operation. It also plays a pivotal role in connecting the communication framework setup by UAV-Net in the remote location to the 5G/6G communication core network. With the right negotiation method, we can modify the system architecture to complete the mission.

While conducting surveillance over the mission area, it is essential that all the UAVs assist in maintaining the topology. This involves maintaining inter-UAV distances, flying formation and flying height of the UAV grid. The synchronisation and coordination is achieved through continuous flow of

Message Queuing Telemetry Transport (MQTT, [46], [47]) commands and instructions between UAVs over wireless network.

IV. MCMV NETWORK TOPOLOGY

In this section, we discuss the framework for multi-UAV network topology to perform surveillance over an inaccessible region. The network topology should be designed so that a small number of UAVs can cover the mission area with no blind spots. To achieve this, we have developed an effective MCMV network topology. There are two stages to the topology development. First, we determine the minimum number of UAVs required for a specific mission area using the field of view (FOV) of the on-board camera. Then, by considering overlapping on the ground, we set the position of UAVs in 3-D space to ensure zero blind spots.

The minimum number of UAVs, for a particular monitoring area, can be decided based on the on-ground coverage area of UAVs. The coverage area of a UAV is defined by the FOV of the on-board camera, with FOV referring to the area captured by the camera at a specific position and orientation in space. Fig. 3 shows the FOV of on-board camera in both horizontal and vertical dimensions. Depending on height of operation λ , the coverage area of a UAV can be given as:

$$C(\lambda) = f_h \cdot f_v \tag{1}$$

where f_h and f_v are the horizontal and vertical FOVs of the on-board camera, respectively, and can be defined as:

$$f_h = 2\lambda \tan\left(\frac{\theta_h}{2}\right), f_v = 2\lambda \tan\left(\frac{\theta_v}{2}\right) \tag{2}$$

where θ_h and θ_v are the horizontal and vertical angles of view (AOV) of the on-board camera, respectively. Both θ_h and θ_v are obtained from the camera specifications such as focal length (F_l), horizontal sensor dimension (S_h), vertical sensor

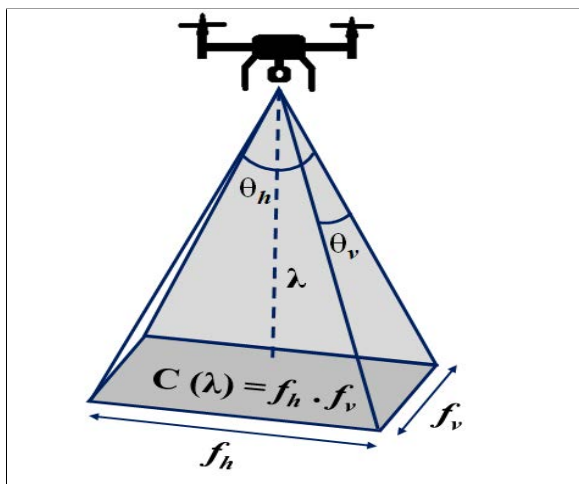


FIGURE 3. Field of view and angle of view of on-board camera.

dimension (S_v) and can be expressed as:

$$\theta_h = 2 \tan^{-1}\left(\frac{S_h}{2F_l}\right), \theta_v = 2 \tan^{-1}\left(\frac{S_v}{2F_l}\right) \tag{3}$$

By substituting (2) and (3) in (1), we obtain the on-ground coverage area of the UAV as:

$$C(\lambda) = \lambda^2 \frac{S_h S_v}{F_l^2} \tag{4}$$

It is evident from equation (4) that for a given camera specifications, the coverage area of UAV depends on the flying height. As the flying height increases, the coverage area also increases. However, at the same time, the quality of surveillance declines. Therefore, it is essential to determine a threshold height that will maintain a balance between the UAV coverage and the quality of surveillance (QoS). The QoS of a UAV at a flying height λ can be defined as:

$$Q(\lambda) = 1 - \mathcal{L}(\lambda), \tag{5}$$

$$\mathcal{L}(\lambda) = a \cdot e^{-\mu \lambda} \tag{6}$$

where $\mathcal{L}(\lambda)$ is the packet loss ratio between the UAV and the target location (i.e. GCS, another UAV, or anchor drone), and can be expressed as an exponential function of flying height λ (that is also the threshold inter-UAV distance) and packet loss exponent μ . The parameter a is a constant ($a > 0$) and μ is the packet loss exponent ($\mu > 0$) that depends on the channel characteristics (channel capacity) and transmission parameters (packet length) [48], [49], [50].

The UAVs form a wireless network called UAV-Net to perform surveillance. We assume that all the UAVs in the UAV-Net have identical camera specifications. As a result, at a given operating height, all UAVs have the same on-ground coverage area. We can establish a minimum number of UAVs to cover the entire monitoring region by carefully placing each UAV. UAVs, on the other hand, are not stationary. A small deviation from the desired position may result in a ground coverage hole. Therefore, when computing the minimum number of UAVs, we consider the coverage area overlapping to ensure zero blind spots. Let $\chi_{i,j}$ denotes the coverage overlapping between UAV i and UAV j . Then, $\chi_{i,j}$ can be defined as:

$$\chi_{i,j} = \begin{cases} 1, & \text{if } (|x_i - x_j| \leq f_h \text{ and } |y_i - y_j| \leq f_v) \\ 0, & \text{otherwise} \end{cases} \tag{7}$$

where (x_i, y_i) and (x_j, y_j) are the horizontal positions of UAV i and j , respectively. The overlap area (covered on ground) for two drones i and j , $\overset{\circ}{A}_{i,j}$, is given as:

$$\overset{\circ}{A}_{i,j} = \begin{cases} (f_h - |x_i - x_j|) \cdot (f_v - |y_i - y_j|), & \text{if } \chi_{i,j} = 1 \\ 0, & \text{otherwise} \end{cases} \tag{8}$$

Let $\overset{\circ}{A} \in \mathbb{R}^{N \times N}$ denotes the overlap matrix that indicates the overlap areas between the UAVs in the UAV-Net. Considering the overlapping on the ground, we aim to achieve zero blind spot by jointly optimizing the number of UAVs and

their positions. We begin the optimization task by estimating the operational height of the UAVs. The operating height is evaluated based on the coverage and QoS requirements. The coverage requirement enforces the UAVs to be deployed at a higher altitude in order to cover larger area on ground. However, the quality of surveillance necessitates placing the UAVs at a lower altitude in order to keep the packetloss under control. To maintain a balance between the two, we estimate a threshold height by equating the QoS to its threshold value, i.e., $Q(\lambda) = Q_{th}$, where Q_{th} indicates the threshold QoS value. After solving, the operational threshold height, $\lambda_{th} = \lambda^*$, is found to be

$$\lambda_{th} = \frac{1}{\mu} \ln \left(\frac{Q_{th}}{a} \right) \quad (9)$$

Assuming that all the UAVs operate at a height $\lambda = \lambda_{th}$, the MCMV topology problem for a surveillance area \mathbf{A} can be formulated as:

$$P1 : \min_{N, X, Y} (\mathbf{A} - NC(\lambda))^2 \quad (10a)$$

$$\text{subject to } NC(\lambda) - \alpha \mathbf{A} \geq \mathbf{A} \quad (10b)$$

$$\sum_{i \in \mathcal{N}} \sum_{j \in \mathcal{N}, j \neq i} \mathbf{A}_{i,j} \leq \alpha \mathbf{A} \quad (10c)$$

$$x_{min} \leq x_i \leq x_{max} \text{ and} \\ y_{min} \leq y_i \leq y_{max}, \forall i \in \mathcal{N} \quad (10d)$$

where $X = \{x_i, \forall i \in \mathcal{N}\}$ and $Y = \{y_i, \forall i \in \mathcal{N}\}$ are the vectors representing the x- and y-coordinate of UAVs in the UAV-Net, respectively. α indicates the overlapping percentage on the ground. The objective function along with the constraint (10b) ensures that the UAV-Net completely covers the surveillance region with no blind spots. The constraint (10c) guarantees that the overall on-ground overlapping regions of UAVs are confined by the threshold area $\alpha \mathbf{A}$. The position bounds of UAVs are defined by (10d). The problem P1 can be approximated by decoupling it into two sub-problems, where the first subproblem optimizes the number of UAVs, and the second subproblem optimizes the placement of the UAVs in the topology.

1) OPTIMIZATION OF NUMBER OF UAVs

For a given overlapping percentage α , the number of required UAVs can be optimized by solving the following optimization problem.

$$P2 : \min_N (\mathbf{A} - NC(\lambda))^2 \quad (11a)$$

$$\text{s.t. } NC(\lambda) - \alpha \mathbf{A} \geq \mathbf{A} \quad (11b)$$

Note that for the above optimization problem, both the objective function and the constraint are convex in nature. As a result, P2 is convex and can be solved by using Lagrange multiplier method. The Lagrange function for the above problem can be expressed as

$$\mathcal{L}(\mathcal{N}, \psi) = (\mathbf{A} - NC(\lambda))^2 - \psi (NC(\lambda) - (\alpha + 1)\mathbf{A}) \quad (12)$$

where ψ is the Lagrange multiplier. By solving the KKT conditions (i.e., $\frac{\partial \mathcal{L}(\mathcal{N}, \psi)}{\partial N} = 0$, and $\frac{\partial \mathcal{L}(\mathcal{N}, \psi)}{\partial \psi} = 0$), we obtain the optimal number of UAVs as

$$N = \left\lceil \frac{(\alpha + 1)\mathbf{A}}{C(\lambda)} \right\rceil \quad (13)$$

where $\lceil \cdot \rceil$ represents the ceiling function that gives the nearest integer value for N .

2) OPTIMIZATION OF PLACEMENT OF UAVs

For a given number of UAVs, the Placement of UAVs can be optimized to achieve zero blind spot on the ground. The placement optimization problem can be formulated as

$$P3 : \min_{X, Y} (\mathbf{A} - NC(\lambda))^2 \quad (14a)$$

$$\text{subject to } \sum_{i \in \mathcal{N}} \sum_{j \in \mathcal{N}, j \neq i} \mathbf{A}_{i,j} \leq \alpha \mathbf{A} \quad (14b)$$

$$x_{min} \leq x_i \leq x_{max} \text{ and} \\ y_{min} \leq y_i \leq y_{max}, \forall i \in \mathcal{N} \quad (14c)$$

Since the position of UAVs are not static, the zero blind spot can be ensured by considering maximum possible overlapping on the ground. i.e., $\sum_{i \in \mathcal{N}} \sum_{j \in \mathcal{N}, j \neq i} \mathbf{A}_{i,j} = \alpha \mathbf{A}$. With this, we propose a successive placement strategy to find a near optimal solution to the problem P3. The fundamental idea is to place the UAVs sequentially in a grid structure starting at one end of the surveillance region and making the way to the other until the entire surveillance region is covered. Each UAV is guaranteed to have an overlapping of $\alpha C(\lambda)$. Assuming that all the UAVs have equal overlapping areas, the overlapping constraint can be written as

$$f_h \Delta v + f_v \Delta h - \Delta h \Delta v = \alpha f_h f_v \quad (15)$$

where Δh and Δv represent the horizontal and vertical overlapping of a UAV, respectively. To simplify the analysis, we consider $\Delta h = \Delta v$. Then, Δh and Δv can be expressed as

$$\Delta h = \Delta v \\ = \left(\frac{f_h + f_v}{2} \right) - \sqrt{\left(\frac{f_h + f_v}{2} \right)^2 - f_h f_v \left(\frac{NC(\lambda)}{\mathbf{A}} - 1 \right)} \quad (16)$$

With this overlapping, the UAVs are arranged in a grid structure. Fig. 4 shows the placement of UAVs over the geographical area under surveillance. The grid consists of rectangular zones, each containing a UAV at its center, with the dimension $f_h \times f_v$. We approximate the closest possible rectangular area with the end points (x_{min}, y_{min}) , (x_{min}, y_{max}) , (x_{max}, y_{max}) , and (x_{max}, y_{min}) , and perform the placement of UAVs over this rectangular area. The number of rows and columns are given as

$$K = \left\lceil \frac{y_{max} - y_{min}}{f_v - \Delta v} \right\rceil \text{ and } L = \left\lceil \frac{x_{max} - x_{min}}{f_h - \Delta h} \right\rceil \quad (17)$$

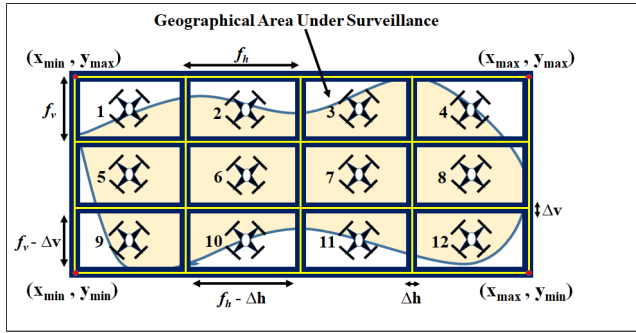


FIGURE 4. Positioning of UAVs in MCMV topology for zero blind spot.

where K and L are the number of rows and columns, respectively. If we assume that the UAVs are placed sequentially starting with (x_{min}, y_{max}) , the x - and y -positions of the UAV in the i^{th} row and j^{th} column are as follows:

$$x_{(i-1)L+j} = \left[x_{ini} + (j-1) \left(f_h - \frac{\Delta h}{2} \right) \right], \text{ and}$$

$$y_{(i-1)K+j} = \left[y_{ini} - (i-1) \left(f_v - \frac{\Delta v}{2} \right) \right] \quad (18)$$

where $x_{ini} = \left[x_{min} + \left(\frac{f_h - \Delta h}{2} \right) \right]$, and $y_{ini} = \left[y_{max} - \left(\frac{f_v - \Delta v}{2} \right) \right]$ are the x - and y -position of UAV in the 1^{st} row and 1^{st} column.

The solutions derived from the two subproblems are only the feasible one, since each subproblem is dealing with only one variable. Therefore, to get closer to the optimal solution, we propose an iterative approach which is summarized in Algorithm 1. To begin, we set $\lambda = \lambda_{th}$ and calculate the number of UAVs required to cover the geographical area with the given overlap. The number of UAVs is then updated for each iteration by updating the position of UAVs. This process is repeated until the number of UAVs equals the number of grid elements.

V. MWL ROUTING PROTOCOL

The UAVs in the UAV-Net record videos of the target location and transmit the information to the GCS through AU over multiple hops. The UAV camera can acquire video at a resolution from a predefined set of supported settings, thereby generating the source traffic at the corresponding data (and packet) rate. Since, multiple UAVs are active (with surveillance data to be transmitted) at the same time, the network can get congested. The UAV buffer stores the video frames while the transmission is ongoing over the 2.4/5GHz WLAN channel established between the neighboring nodes in the UAV-Net. In order to address congestion and effective surveillance video transmission from the UAV-Net, we propose an efficient MWL routing protocol that distributes traffic evenly among all the available links to control network congestion. The routing protocol works in two stages. The first stage is route discovery, in which the UAVs in the UAV-Net find multiple node disjoint minimum hop pathways to the AU. Then,

Algorithm 1 Iterative Algorithm for Optimal MCMV Topology

Require: $\mu, a, Q_{th}, S_h, S_v, F_l, A, \alpha$

Ensure: λ_{th}, N, X , and Y

- 1: Determine λ_{th} using Eq. (9)
- 2: Update $C(\lambda)$ according to Eq. (4) for $\lambda = \lambda_{th}$
- 3: For given α , update N according to Eq. (13)
- 4: **repeat**
- 5: Update Δh and Δv according to Eq. (16)
- 6: Update K and L according to Eq. (17)
- 7: **for** $i = 1$ to K **do**
- 8: **for** $j = 1$ to L **do**
- 9: Update $x_{(i-1)L+j}$ and $y_{(i-1)L+j}$ according to Eq. (18)
- 10: **end for**
- 11: **end for**
- 12: **if** $KL > N$ **then**
- 13: $N \leftarrow N + 1$
- 14: **else**
- 15: $N \leftarrow N - 1$
- 16: **end if**
- 17: **until** $KL = N$

in the next stage, the UAVs convey their information to the AU by balancing the load over these multiple pathways. In the event of congestion the camera acquisition video resolution is switched to a lower-level thereby reducing the number of packets generated from the source.

A. ROUTE DISCOVERY

The primary requirement of the routing protocol is to find various node disjoint minimum hop pathways from source nodes (UAVs in the grid) to the destination node (AU). In order to accomplish this, the source node transmits a route discovery control message. The format of the route discovery control message is displayed in Fig. 5. The message is flooded (broadcast) network-wide from source node to the destination node. During the process, the intermediate node may receive multiple copies of the same control message through different pathways. In case a few route discovery messages are lost or some possible paths are missing, route discovery control message broadcast helps in finding the next best feasible set of paths from the source to the destination. The intermediate node selects the one with least hop count value and discards the others. The AU examines all the received control messages and selects the one with the fewest hops. The selected message is then compared to other control messages for node disjointness. This results in selection of two node disjoint

Message ID	Destination Address(DA)	Source Address(SA)	Cumulative weight(W)	Path (P)	Hop Count
------------	-------------------------	--------------------	----------------------	----------	-----------

FIGURE 5. Control message for route discovery.

pathways for the edge node and three node disjoint pathways for the inner node, corresponding to the neighboring nodes with links on paths to the destination, which is shown in Fig. 6. The AU assigns a unique sequence number to each selected pathways and forwards a route reply message to the source node. Fig. 7 shows the format for the reply control message. The source node creates a routing table after receiving the route reply message.

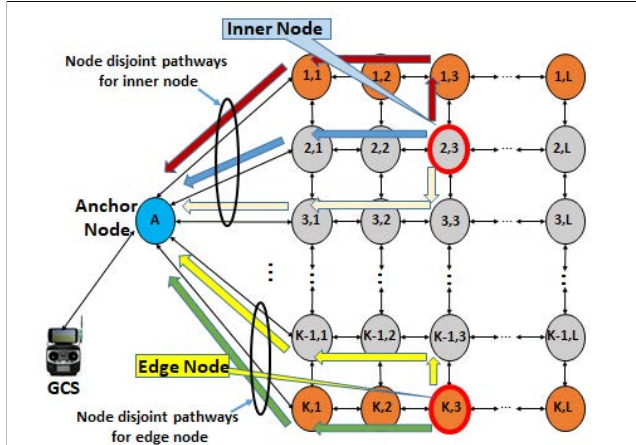


FIGURE 6. Minimum hop node disjoint pathways: Edge node and inner node.

Seq. No.	Destination Address(DA)	Source Address(SA)	Path weight(W)	Path (P)	Hop Count

FIGURE 7. Format for route reply control message.

Routing state information stored at each UAV consists of the path information (i.e. control messages with least hop count at the intermediate node) between source-destination pairs. This does not introduce communication overhead during the transmission of the surveillance video GOP (group of pictures) by relying on the routing information already available from the previous link update broadcast received from a source node.

B. DATA FORWARDING AND CONGESTION CONTROL

We use a unique weighted load balancing (WLB) mechanism for data forwarding, in which the data forwarding at source node is performed by balancing the load among multiple pathways to the destination. The path weight, which corresponds to the data traffic on the path, can be utilised to determine the load distribution on the path. Therefore, in order to alleviate network congestion, the WLB routes more traffic on the path with less weight and less traffic on a more weighted path. The details of data forwarding over the UAV-Net using MWL routing is as follows.

In MWL routing, the source node can either be an edge node or an inner node. We use the variable P_i to characterize the source node i . P_i can take two possible values: 0 or 1.

$P_i = 0$ for edge node and $P_i = 1$ for inner node. Let $\mathcal{P} = \{P_i, \forall i \in \mathcal{N}\}$ be the description of all the source nodes. The data traffic for an edge node must be sent over two node disjoint paths, whereas it must be distributed over three node disjoint paths for the inner node. The amount of data flow along each path is decided by utilising the path weight, which can be calculated by adding the associated link weights. The link weights are set as the link capacity (i.e. the maximum traffic the link can support). Assume that the network has M links, denoted as l_0, l_1, \dots, l_M , which can be given as $\mathcal{M} = \{1, 2, \dots, M\}$. The collection of link weights can be expressed as $\mathcal{W} = \{w_k, \forall k \in \mathcal{M}\}$, where w_k denotes the weight corresponding to the link k . Assume that the association between the source node i and the link k is represented by $\sigma_{j,k}^i$. Then, $\sigma_{j,k}^i$ can be defined as

$$\sigma_{j,k}^i = \begin{cases} 1, & \text{if node disjoint path } j \text{ of source node } i \text{ is} \\ & \text{associated with link } k \\ 0, & \text{if node disjoint path } j \text{ of source node } i \text{ is} \\ & \text{not associated with link } k \end{cases} \quad (19)$$

Let $A = \{\sigma_{j,k}^i, \forall i \in \mathcal{N}, j \in \{1, 2, 3\}, \text{ and } k \in \mathcal{M}\}$ be the association matrix reflecting the association between the nodes and links in the network. Then, the path weight of the node disjoint path j of the source node i can be evaluated as

$$W_j^i = \sum_{k \in \mathcal{M}} \sigma_{j,k}^i \cdot w_k \quad (20)$$

The traffic ratio corresponding to path j can be calculated as

$$r_j^i = \begin{cases} \frac{W_j^i}{\sum_{m=1}^2 W_m^i}, & \text{if } P_i = 0 \\ \frac{W_j^i}{\sum_{m=1}^3 W_m^i}, & \text{if } P_i = 1 \end{cases} \quad (21)$$

The UAVs in the UAV-Net are the sources that are generating data traffic, R , the volume of which depends on the surveillance video acquisition resolution. A high resolution video corresponds to more number of packets to be transmitted over the network. The source video consists of frames. A set of frames, also known as the group of pictures (GOP), that are captured per second get encoded into a video stream. The video stream is transmitted in the UAV-Net in the form of packets. The traffic distribution can be performed by following load balancing mechanism, in which more traffic is forwarded over the path with less weight and less traffic is forwarded over the path with higher weight. The details of data traffic distribution is provided in Algorithm 2. This algorithm is periodically executed after transmission of each surveillance video GOP thereby governing re-routes and traffic distribution updates in each GOP transmission period. The association matrix A is used in updating path weight, W_j^i , according to (20). Every time there is a traffic flow, associated with the surveillance video GOP, on the path, the weight of the path increases. To update the path weight, the source node broadcasts a link update control message at the end of each

Algorithm 2 WLB Algorithm for Traffic Distribution**Require:** $\mathcal{W}, A, R, T, P, N$ **Ensure:** Traffic distribution of node disjoint pathways

```

1: for  $i \leftarrow 1$  to  $N$  do
2:   if ( $P_i = 0$ ) then
3:     Update  $W_1^i$  and  $W_2^i$  according to Eq. (20) using  $A$ 
4:     Update  $r_1^i$  and  $r_2^i$  according to Eq. (21)
5:      $p1 = \arg \max(r_1^i, r_2^i)$ 
6:      $p2 = \arg \min(r_1^i, r_2^i)$ 
7:     if  $((\min(r_1^i, r_2^i) \times R) \leq T)$  then
8:       Data traffic on path  $p1(D_1^i) = \min(r_1^i, r_2^i) \times R$ 
9:     end if
10:    if  $((\max(r_1^i, r_2^i) \times R) \leq T)$  then
11:      Data traffic on path  $p2(D_2^i) = \max(r_1^i, r_2^i) \times R$ 
12:    end if
13:    else if ( $P_i = 1$ ) then
14:      Update  $W_1^i, W_2^i$  and  $W_3^i$  according to Eq. (20)
using  $A$ 
15:      Update  $r_1^i, r_2^i$  and  $r_3^i$  according to Eq. (21)
16:       $p1 = \arg \max(r_1^i, r_2^i, r_3^i)$ 
17:       $p2 = \arg \min(r_1^i, r_2^i, r_3^i)$ 
18:       $p3 = \{1, 2, 3\} - \{p1, p2\}$ 
19:      if  $((\min(r_1^i, r_2^i, r_3^i) \times R) \leq T)$  then
20:        Data traffic on path  $p1(D_1^i) = \min(r_1^i, r_2^i, r_3^i) \times$ 
 $R$ 
21:      end if
22:      if  $((\max(r_1^i, r_2^i, r_3^i) \times R) \leq T)$  then
23:        Data traffic on path  $p2(D_2^i) =$ 
 $\max(r_1^i, r_2^i, r_3^i) \times R$ 
24:      end if
25:      if  $((R - (D_1^i + D_2^i)) \leq T)$  then
26:        Data traffic on path  $p3(D_3^i) = R - (D_1^i + D_2^i)$ 
27:      end if
28:    end if
29: end for

```

GOP transmission (i.e. per second) with the remaining data of the GOP piggybacked with the control message. All the nodes in the network update their routing table by recalculating the new path weight to the destination. The selected message with link update control information is forwarded by the intermediate node to the AU on all interfaces except the one on which it is being received. The path weight update for source node i can be given as

$$W_j^i[\text{new}] = W_j^i[\text{old}] + W_{j,\text{inc}}^i \quad (22)$$

where $W_{j,\text{inc}}^i$ denotes the increase in the weight of path j of source node i and is defined as

$$W_{j,\text{inc}}^i = \begin{cases} n_i \times D_j^i, & \text{if path } j \text{ is the shortest one} \\ (n_i + 1) \times D_j^i, & \text{Otherwise} \end{cases} \quad (23)$$

where n_i is the number of hop count from source node i to the destination (i.e. anchor drone), and D_j^i is the data traffic distribution on path j of source node i .

Before transmitting through any path, the source node inspects the path condition. For this, it has to check two threshold conditions: (a) Path break threshold, and (b) Congestion threshold. The path break threshold and the congestion threshold for the edge node are set to $n_i T$ and $2T$, respectively, whereas the path break threshold and congestion threshold for the inner node are $(n_i + 1)T$ and $3T$, respectively, where T indicates the highest data rate supported by each link. If a source node finds the weight of any node disjoint path above the path break threshold value, it forwards the entire traffic through other available paths. A re-route discovery is conducted if the node finds all its disjoint paths have weights above the path break value. In case of congestion, the nodes wait for the directions from higher layer and store the video in the buffer in the meantime.

In such a scenario, when congestion occurs, the video acquisition module on the UAVs switch to a lower resolution. This reduces the amount of data (i.e. number of packets) to be transmitted from a given source, i.e. R .

Video transmission is tolerant to packet losses to a certain extent [51], [52]. A packet loss of upto 4% is acceptable for video streaming application in terms of the perceptual video quality [53], [54]. The MCMV topology has the inter-UAV distance and UAV-GCS distance selected to be less than the threshold that prevents the packet loss to be greater than the acceptable limits. Furthermore, in the event of congestion, with MWL routing scheme, the source data (and packet) rate is reduced to prevent the packet loss from exceeding the acceptable limit.

VI. RESULTS AND ANALYSIS**A. TESTBED DETAILS**

A Raspberry Pi 3 B+ companion computer is used on board to assist in the surveillance along with mission planning software. The UAV's movement is guided by the flight controller. In order to facilitate packet forwarding, the UAV includes two WLAN adapters, one internal and one external, which are shown in Fig. 8. The internal WLAN adapter is used to create the Access Point (AP), while the external WLAN adapter is utilized to connect the UAV as a client to the AP created by an adjacent UAV. The hardware and software components necessary to set up a UAV are listed in Table 3. It is important to note that, we have used two power supplies (as listed in Table 3) in our UAV assembly, one for the UAV flying operation (motor, controller), and the other for communication framework (Raspberry Pi board). The proposed MWL routing scheme focuses to efficiently transmit the surveillance video from the UAV to the GCS with a reduced energy consumption in the associated communication that effectively improves the UAV-Net lifetime.

We use wireless LAN (WLAN) as the primary technique for connecting UAVs to the GCS. Fig. 9 shows an experimental setup to illustrate WLAN-based communication between the UAV 1 and the GCS. The AU includes two WLAN adapters: internal WLAN (WLAN 0) and external WLAN

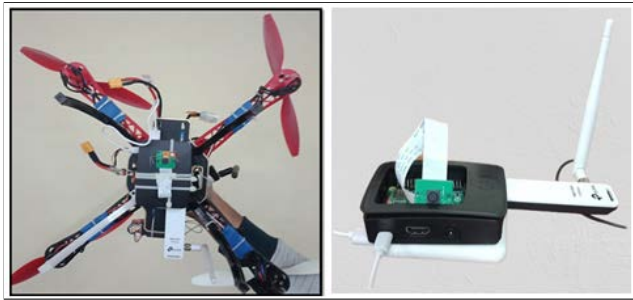


FIGURE 8. An image of anchor drone with raspberry Pi 3 B+ with external Wifi adapter.

TABLE 3. Hardware and Software components of UAV.

HARDWARE		
Component	Role	Qty
Pixhawk px 4 2.4.8 with GPS	Flight Controller	1
Q450 Quadcopter Frame	Frame of UAV	1
Raspberry Pi 3 Model B+	Companion computer	1
TP-Link TL-WN722N	External Wi-fi adapter	1
DYS SimonK 30A Speed Controller ESC	Electronic speed Controller	4
KV980 II Motor	UAV motors	4
Camera Module	surveillance camera	1
Lipo Battery 3300mAh 14.8V 25C 4S1P	Power supply for UAV	1
5000mAh Power bank for Raspberry Pi	Power supply	1
SOFTWARE		
Raspbian Stretch	OS	-

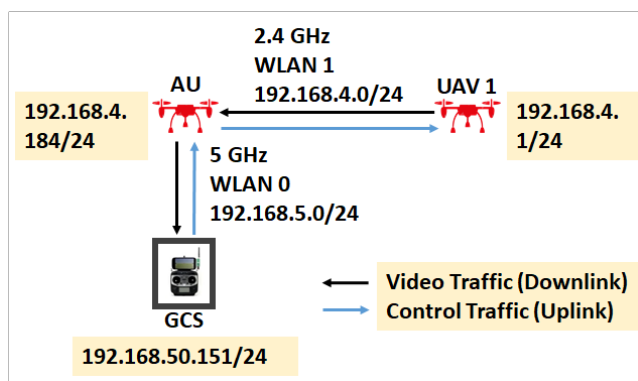


FIGURE 9. Anchor UAV relaying video traffic to GCS.

(WLAN 1). WLAN 0 creates an access point (AP) with IP 192.168.5.0/24, while WLAN 1 connects the AU as a client to AP 192.168.4.0/24 created by UAV 1. To avoid interference, the anchor UAV is configured on 5 GHz frequency band, while the UAV 1 is configured on 2.4 GHz band. Since the framework is designed for a remote inaccessible region, the interference within the 2.4 and 5 GHz band is limited and is only caused due to the UAV-Net transmissions.

B. MCMV TOPOLOGY EVALUATION

We start the topology evaluation by validating the coverage with zero blind spots. To support this, we consider a

TABLE 4. Experimental validation of coverage area at various flying heights.

Flying heights (m)	Mathematically calculated Coverage area (m ²)	Actual Coverage Area (m ²)	Accuracy (%)
5.72	26.009	30	85
10.38	85.64	99.5	83.81
15.72	196.45	232.0	82

UAV with on-board camera specifications of $F_l = 3.60$ mm, $S_h = 3.76$ mm, and $S_v = 2.74$ mm. The UAV is configured to fly at three different flying heights of 5 m, 10 m, and 15 m, and the coverage area is measured for each variation. A comparison between the actual covered area and mathematically calculated values is given in Table 4. The result shows that the actual covered area is always greater than the calculated value. Therefore, if we keep the inter UAV distances in both horizontal and vertical directions below f_h and f_v , respectively, there will always be overlap between the two contiguous fields of view of adjacent drones. This guarantees zero blind spots even if drones deviate slightly from their intended positions.

After validating zero blind spot, we investigate the effect of flying altitude on topology development. For this, we consider different geographic regions and evaluate the average number of UAVs required at three different flying heights of 50 m, 75 m, and 100 m. Fig. 10 shows the coverage area vs average number of UAVs required at different flying heights. It is observed that higher the flying height of the UAVs, more is the on ground coverage area and hence, lesser number of UAVs are needed to cover a geographical area. On the other hand, UAVs flying at lower height cover lesser geographical area on ground, hence more UAVs are needed to cover the same area. So, by customizing the UAVs to fly at a larger height, we can achieve the coverage with minimum possible UAVs. However, larger height degrades the service quality. Therefore, we decide a threshold height (λ_{th}) in order to optimize the number of UAVs required to cover a mission area.

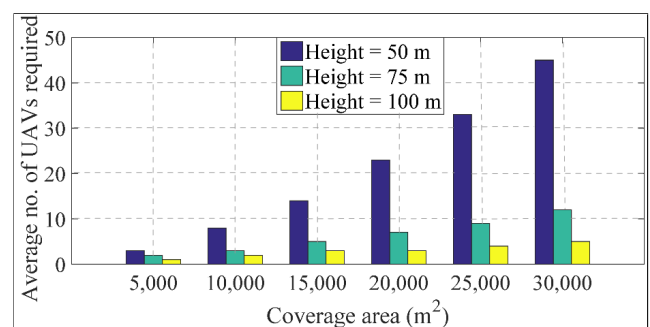


FIGURE 10. Average no. of drones required for surveillance of a given coverage area.

The threshold height, λ_{th} , is determined by analyzing the quality of video received at GCS from the AU. We configure

the AU to perform video streaming at various flying heights and evaluate the packet loss at GCS using the wireshark application. The percentage of packet loss in video transmission from UAV at different flying heights to GCS is experimentally obtained using Wireshark tool traces over multiple instances. The experimental packet loss at different flying heights and the corresponding analytical function given by (6) is shown in Fig. 11. The parameters $a = 0.012$ and $\mu = 0.012$ in (6) correspond to less than 0.01 root mean square error between the experimental and analytical packet loss percentage. It is observed that at 100 m, the packet loss is 4% while the video quality at GCS is rated “acceptable” in Mean Opinion Score (MOS). Beyond 100 m, the packet loss increases to an undesirable level of more than 4%. As a result, the UAV’s threshold flying height $\lambda_{th}h$ is set to be 100 m for optimum performance.

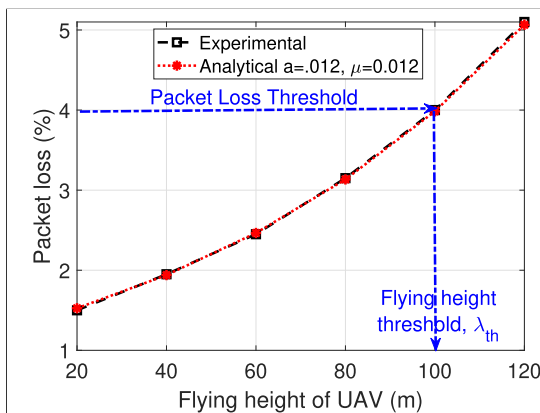


FIGURE 11. Experimental and analytical packet loss evaluation at GCS for video streaming from UAV.

We also investigate the effect of coverage area overlap on topology development. We consider a surveillance area of $20000 m^2$ and evaluate the average number of UAVs required to cover the area with various overlapping percentages. The evaluation results are shown in Fig. 12. It is found that the number of required UAVs increases with overlapping. This is because overlap reduces the effective coverage, necessitating more number of UAVs to cover the same area. This effect is more prominent at low altitude than at high altitude. Therefore, we can configure the UAVs to fly at larger heights to allow greater overlapping in order to ensure zero blind spot during surveillance.

Fig. 13 compares the proposed MCMV topology with the existing constrained coverage (CC) topology [17], [20]. Both the topologies are compared in terms of average number of UAVs required for surveillance. We consider two different simulation scenarios. In Fig. 13 (a), we consider a mission area of $20000m^2$ and evaluate the average number of UAVs required for different flying heights, whereas in Fig. 13 (b), we fix the flying height at 50 m, and evaluate the average number of UAVs needed for different coverage area. In both the cases, the proposed MCMV topology outperforms the CC

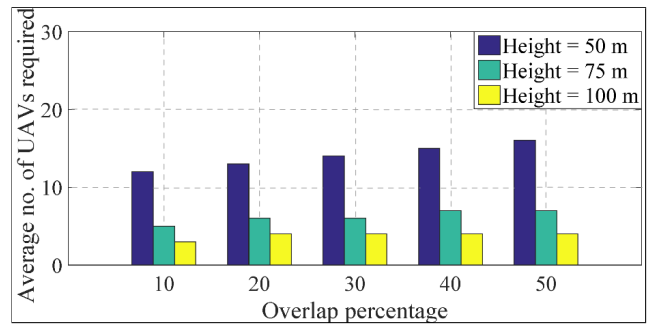


FIGURE 12. Number of UAVs variation w.r.t coverage area overlapping.

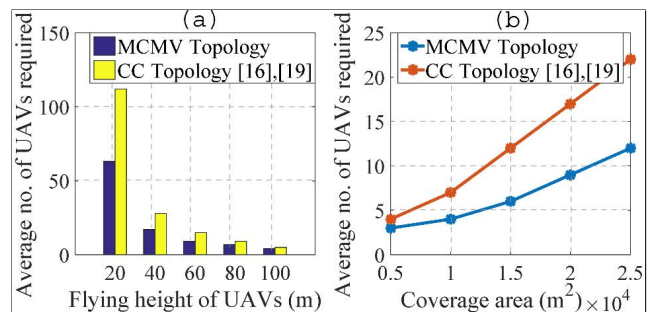


FIGURE 13. Number of UAVs in MCMV as compared to CC [17], [20] topology.

topology by reducing the number of UAVs by 74.65% (on average).

C. MWL ROUTING PROTOCOL EVALUATION

The MWL routing protocol is evaluated by performing extensive simulations in MATLAB. The simulations are performed for the network shown in Fig. 14 and the parameters for simulation are listed in Table 5. We have performed Monte-Carlo simulation with more than 100 instances of network scenario and 95% confidence interval.

We have evaluated the performance of our proposed MWL routing scheme in comparison with SMURF [39], SPA [43], [44], and LMP-DSR [34]. In addition to being light-weight, link-existence based, and load-balanced, similar to SPA, our

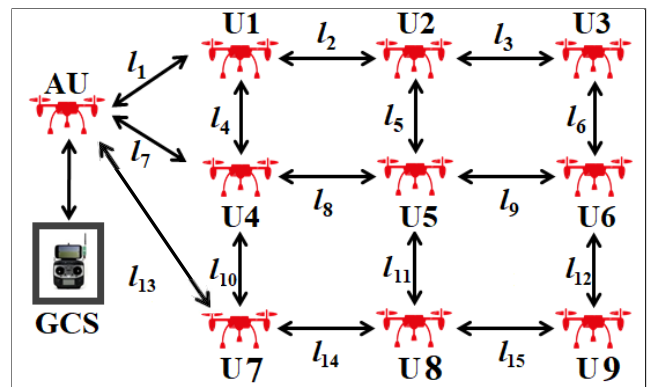
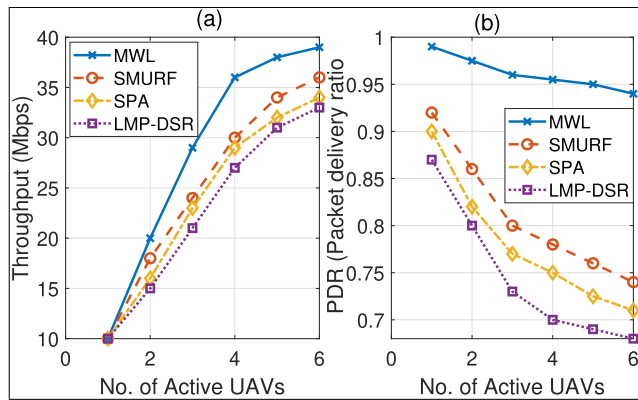


FIGURE 14. Topology for simulation of MWL routing.

TABLE 5. Simulation parameters for MWL routing.

Parameter	Value
Number of Nodes	10
Number of transmitting Nodes	6
Traffic at each Node	2-10 Mbps
Max Traffic Supported by each Link	21 Mbps
Onboard Camera resolutions	1920 × 1080, 1280 × 720, 640 × 480
Number of Packets per video GOP per sec (F_{no})	2k – 4k (approx)
Packet Size	1500 bytes
Inter-UAV distance	100 m

**FIGURE 15.** Throughput and PDR comparison of MWL with SMURF, SPA, and LMP-DSR.

MWL routing protocol, additionally, is application aware and performs simultaneous multipath packet delivery with congestion control over a QoS-aware optimal MCMV topology. Although SMURF uses simultaneous multi-path packet delivery, it performs packet replication on the multiple paths to improve packet delivery ratio. However, our proposed MWL routing protocol gains by simultaneously transmitting a weighted distribution of packets on the multiple node disjoint paths in a QoS-aware MCMV topology. All these routing protocols are compared in terms of QoS parameters such as throughput, PDR, end-to-end delay, packet loss rate, and energy efficiency.

1) THROUGHPUT AND PACKET-DELIVERY-RATIO (PDR)

Fig. 15 shows the comparative performance of MWL, SMURF, SPA, and LMP-DSR routing schemes in terms of throughput and PDR. It is seen from Fig. 15(a) that all the routing protocols attain the same throughput (10 Mbps) when there is only one active node. However, as the number of transmitting nodes increases, the MWL routing provides higher throughput by 13.16%, 19.14%, and 25.55% (on average) than the SMURF, SPA, and LMP-DSR routing schemes, respectively. Also, we can see from Fig. 15(b) that the PDR of all the routing methods decreases with increase in the number of active transmitting UAVs but the proposed MWL routing scheme has a PDR greater than other schemes, 0.94 even with

6 active UAVs. the MWL routing provides higher PDR by 18.72%, 23.42%, and 29.08% (on average) than the SMURF, SPA, and LMP-DSR routing schemes, respectively.

This is because in LMP-DSR and SPA, the source only transmits via the path selected (by the routing scheme) from amongst the multiple paths available. This results in certain links like l_1 , l_7 , and l_{13} (which serve as the interface between the AU and UAV-Net) to support a maximum of three simultaneous video transmission by three UAVs. This puts a limitation on the system throughput and PDR. However, such limitation is avoided in MWL routing through load balancing. Here, the source node balances the load among multiple node disjoint paths, thus allowing links l_1 , l_7 , and l_{13} to accommodate more than three simultaneous video transmissions. Since SMURF performs packet replication on the multiple paths to improve PDR, it is not effective in our scenario with limited capacity links and many transmitting nodes. In MWL, the network can allow multiple simultaneous video transmissions with its source adaptive congestion control strategy. When the number of active drones increases, congestion occurs which is avoided by reducing the video resolution (data/ packet rate). In this situation, the network supports multiple UAVs to transmit simultaneously. Thus, the throughput and PDR achieved by the network to be higher (19.38% and 23.74%, on average, respectively) with MWL scheme as compared to the other routing protocols.

2) END-TO-END DELAY

The effectiveness of MWL routing is also evaluated by comparing the end-to-end delay performance of MWL in comparison with SMURF, SPA, and LMP-DSR. We consider the source video resolution set as {1080p, 720p, 480p}, where transmission of a 1080p corresponds to a true colour HD resolution from source node to the Anchor node. The transmission is based on group of picture (GOP) that is a set of video frames encoded collectively in a second. We compute the delay at the destination end for the GOP (30 frames in a GOP for frame rate = 30fps). The simulation scenario is shown in Fig. 14 and the parameters used for simulation settings are listed in Table 5.

With the above parameters, the free space packet propagation delay for a link distance of 100 m is found to be 4ms. Then, the propagation delay for a video frame to reach the destination can be calculated as

Delay

$$= \begin{cases} \sum_{i=1}^{F_{no}} n_h^i \times P_d, & \text{for SMURF, SPA, LMP-DSR} \\ (n_h + 1) \times P_d \times \frac{F_{no}}{n_{disjoint}}, & \text{for MWL} \end{cases} \quad (24)$$

where n_h is the number of hop count from source UAV to the Anchor UAV, n_h^i is the number of hop count along the path selected for packet i , P_d is the packet propagation delay for each hop (4 ms), F_{no} is the number of packets in the video GOP (per sec), and $n_{disjoint}$ is the number of node

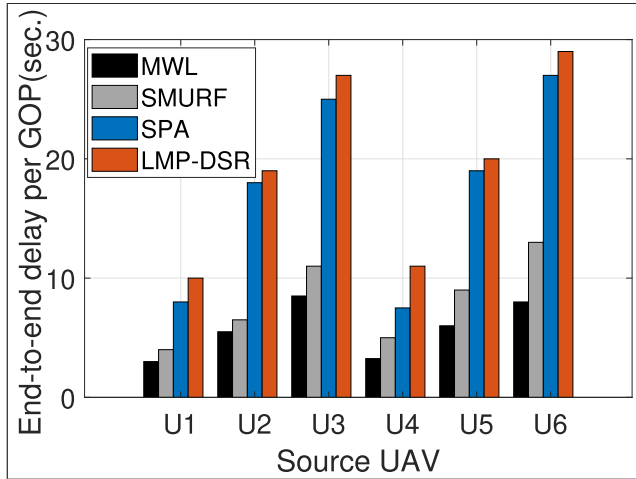


FIGURE 16. Delay Comparison of MWL with SMURF, SPA, and LMP-DSR.

disjoint path selected at source node for data transmission. Distinctively, in MWL the video GOP packets are transmitted on node disjoint paths simultaneously, unlike SMURF that performs packet replication and LMP-DSR (as well as SPA) that transmits using a single selected path (from possible multiple paths). The delay comparison of MWL with SMURF, SPA, and LMP-DSR routing schemes is shown in Fig. 16.

The MWL routing has a lower end-to-end delay by 29.38%, 67.22%, and 70.47%, on average, in comparison to the SMURF, SPA, and LMP-DSR routing schemes. In SPA and LMP-DSR, each packet is delivered along the independently selected path (from the set of multiple paths available in the route cache) to the destination, whereas all these video packets corresponding to a video frame are proportionally distributed simultaneously over multiple node disjoint paths in case of MWL routing. In SMURF packet replication on the multiple paths increases the volume of packets in the network resulting in congestion with many active UAVs in the network. However, our proposed MWL routing protocol simultaneously transmits a weighted distribution of packets on the multiple node disjoint paths. As a result, with MWL routing, the effective number of packets transmitted over each path is lower, which ultimately reduces the end-to-end delay. We also notice that nodes at the same distance from the anchor drone experience the same amount of delay. As the distance increases, the end-to-end delay also increases.

3) PACKET LOSS

The experimental packet loss analysis (Fig. 11) in the topology evaluation has shown that a distance of 100 m results in a packet loss of 4 %, which is the maximum acceptable limit. So, we set the inter-UAV distances to 100 m in the scenario shown in Fig. 14 and analyze the packet loss of MWL routing by varying the number of transmitting nodes with the other simulation settings given in Table 5. Fig. 17 shows packet loss comparison of MWL with SMURF, SPA, and LMP-DSR. It is evident from the figure that MWL

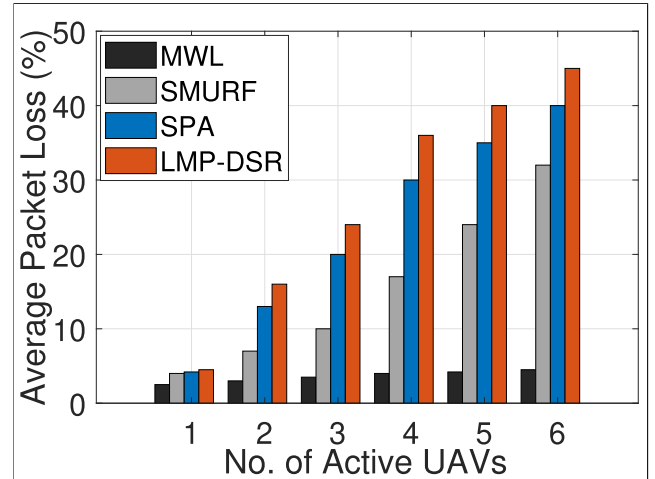


FIGURE 17. Packet Loss percentage comparison of MWL with SMURF, SPA, and LMP-DSR.

routing has lesser packet loss percentage by 76.91%, 84.74%, and 86.89%, on average in comparison to SMURF, SPA, and LMP-DSR routing schemes, respectively. This is attributed to the application-aware and simultaneous multi-path load balanced packet transmission in MWL routing. Load-balancing and source adaptive congestion control enables MWL routing to dynamically balance traffic throughout the network and reduce average packet loss percentage in the UAV-Net.

4) ENERGY EFFICIENCY

The energy efficiency of a routing protocol can be evaluated in terms of nodes' residual energy and network lifetime. The residue energy of a node is calculated using the equation below.

$$E_{res} = E_{ini} - E_{con} \tag{25}$$

where E_{ini} is the initial energy available at the node and E_{con} is the total energy consumed by the node. E_{ini} can be determined from the battery specifications using the relation $Energy(J) = Voltage(V) \times Charge(mA.h) \times 3.6$. To evaluate E_{con} , we use the first order energy consumption model [55]. This is a popular model used for evaluating the WSN routing protocols. According to this model, the energy consumed by a node for sending and receiving m bit data is given as:

$$E_{Tx}(m, d) = m(E_{elec} + E_{amp}.d^2) \tag{26}$$

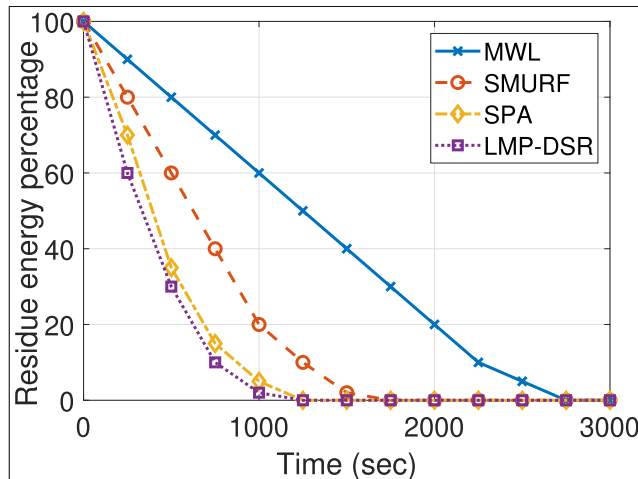
$$E_{Rx}(m, d) = m.E_{elec} \tag{27}$$

where E_{Tx} and E_{Rx} are the energy consumed during data transmission and reception respectively, E_{elec} denotes the single bit energy consumption at the transmitter and receiver circuits, E_{amp} represents the single bit energy consumption at the amplifier circuit, and d is the distance over which information is transmitted. The total energy consumed by the node is calculated as

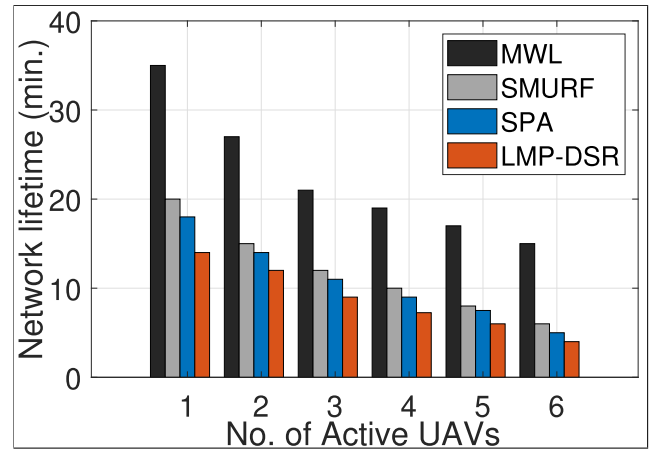
$$E_{con} = E_{Tx} + E_{Rx} \tag{28}$$

TABLE 6. Parameters for calculating residue energy of node.

Parameter	Value
Onboard Battery specification	16V, 5000 mAh
Inter-UAV distance	100 m
Packet Size	1500 bytes
E_{elec}	50 nJ/bit
E_{amp}	10 PJ/bit/m ²

**FIGURE 18.** Energy efficiency comparison of MWL with SMURF, SPA, and LMP-DSR in terms of residue energy percentage.

For evaluation, we consider the scenario shown in Fig. 14 with settings as given in Table 5 and we evaluate the residue energy at UAVs. The UAVs U1, U4, and U7 are the ones that deplete faster than others and play a key role in deciding the network lifetime. Assuming that all the UAVs have the same initial energy, we run the routing algorithms for 3000 simulated seconds. The parameters utilised in the simulation are listed in Table 6. Figs. 18 and 19 compares the energy efficiency of MWL with SMURF, SPA, and LMP-DSR routing. Fig. 18 compares the residue energy percentage of the routing schemes while Fig. 19 shows the comparison of network lifetime. It is evident from the figure 19 that the MWL routing algorithm is more energy efficient in terms of residue energy percentage than SMURF, SPA, and LMP-DSR routing schemes. The residue energy of MWL is 43.78%, 59.46%, and 63.60% higher (on average) than SMURF, SPA, and LMP-DSR routing schemes, respectively. With MWL routing, the network life time is improved by 47.01%, 51.87%, and 61.01% (on average) in comparison with SMURF, SPA, and LMP-DSR routing schemes, respectively. Even though, we have evaluated the energy efficiency performance of our proposed MWL scheme with respect to other protocols for settings corresponding to our hardware design, it is equivalently applicable to any generic UAV network system as well. Thus, MWL routing scheme can be effectively utilised for surveillance in remote (inaccessible) regions for a longer duration using UAV-Net.

**FIGURE 19.** Energy efficiency comparison of MWL with SMURF, SPA, and LMP-DSR in terms of Network lifetime with increase in number of transmitting nodes.

VII. CONCLUSION AND FUTURE WORK

In this work, we have introduced an efficient UAV-assisted surveillance system to facilitate surveillance in remote inaccessible locations. In particular, we have developed a QoS-aware topology, that minimizes the number of UAVs required to conduct surveillance with zero blind spots. We have also determined the threshold operational height in order to keep the packet loss within the acceptable limit. Then, for reducing network congestion, we have proposed an effective and efficient application-aware load balancing-based routing strategy. Finally, we assess the performance effectiveness of the suggested surveillance system through extensive simulations. We have shown that the proposed surveillance system accomplishes zero blind spot surveillance with lesser number of UAVs and reduced energy consumption, while offering higher throughput and lesser end-to-end delay when compared to the existing state-of-the-art mechanisms in literature.

Further extension of the proposed framework will incorporate synchronisation aspects of UAV swarm in order to assure collision avoidance during surveillance. The interference can be further reduced through dynamic channel allocation in the UAV-Net.

REFERENCES

- [1] R. Ke, Z. Li, S. Kim, J. Ash, Z. Cui, and Y. Wang, "Real-time bidirectional traffic flow parameter estimation from aerial videos," *IEEE Trans. Intell. Transp. Syst.*, vol. 18, no. 4, pp. 890–901, Apr. 2016.
- [2] Y. Qu, L. Jiang, and X. Guo, "Moving vehicle detection with convolutional networks in UAV videos," in *Proc. 2nd Int. Conf. Control, Autom. Robot. (ICCAR)*, Apr. 2016, pp. 225–229.
- [3] R. L. Finn and D. Wright, "Unmanned aircraft systems: Surveillance, ethics and privacy in civil applications," *Comput. Law Secur. Rev.*, vol. 28, no. 2, pp. 184–194, 2012.
- [4] A. Merwaday and I. Guvenc, "UAV assisted heterogeneous networks for public safety communications," in *Proc. IEEE Wireless Commun. Netw. Conf. Workshops (WCNCW)*, Mar. 2015, pp. 329–334.
- [5] K. Hartmann and K. Giles, "UAV exploitation: A new domain for cyber power," in *Proc. 8th Int. Conf. Cyber Conflict (CyCon)*, Jun. 2016, pp. 205–221.
- [6] K. G. Panda, S. Das, D. Sen, and W. Arif, "Design and deployment of UAV-aided post-disaster emergency network," *IEEE Access*, vol. 7, pp. 102985–102999, 2019.

- [7] C. Pu and L. Carpenter, "To route or to ferry: A hybrid packet forwarding algorithm in flying ad hoc networks," in *Proc. IEEE 18th Int. Symp. Netw. Comput. Appl. (NCA)*, Cambridge, MA, USA, Sep. 2019, pp. 1–8.
- [8] T. Wall and T. Monahan, "Surveillance and violence from afar: The politics of drones and liminal security-scapes," *Theor. Criminol.*, vol. 15, no. 3, pp. 239–254, 2011.
- [9] J. Gu, T. Su, Q. Wang, X. Du, and M. Guizani, "Multiple moving targets surveillance based on a cooperative network for multi-UAV," *IEEE Commun. Mag.*, vol. 56, no. 4, pp. 82–89, Apr. 2018.
- [10] H. Kim, L. Mokdad, and J. Ben-Othman, "Designing UAV surveillance frameworks for smart city and extensive ocean with differential perspectives," *IEEE Commun. Mag.*, vol. 56, no. 4, pp. 98–104, Apr. 2018.
- [11] S. Qazi, A. S. Siddiqui, and A. I. Wagan, "UAV based real time video surveillance over 4G LTE," in *Proc. Int. Conf. Open Source Syst. Technol. (ICOSST)*, Dec. 2015, pp. 141–145.
- [12] E. Semsch, M. Jakob, D. Pavlicek, and M. Pechoucek, "Autonomous UAV surveillance in complex urban environments," in *Proc. IEEE/WIC/ACM Int. Joint Conf. Web Intell. Intell. Agent Technol.*, vol. 2, Sep. 2009, pp. 82–85.
- [13] A. Al-Hourani, S. Kandeepan, and S. Lardner, "Optimal LAP altitude for maximum coverage," *IEEE Wireless Commun. Lett.*, vol. 3, no. 6, pp. 569–572, Dec. 2014.
- [14] M. Mozaffari, W. Saad, M. Bennis, and M. Debbah, "Drone small cells in the clouds: Design, deployment and performance analysis," in *Proc. IEEE Global Commun. Conf. (GLOBECOM)*, Dec. 2015, pp. 1–6.
- [15] S. Barick and C. Singhal, "Multi-UAV assisted IoT NOMA uplink communication system for disaster scenario," *IEEE Access*, vol. 10, pp. 34058–34068, 2022.
- [16] D.-Y. Kim and J.-W. Lee, "Topology construction for flying ad hoc networks (FANETS)," in *Proc. Int. Conf. Inf. Commun. Technol. Converg. (ICTC)*, Oct. 2017, pp. 153–157.
- [17] H. Shakhathreh, A. Khreishah, J. Chakareski, H. B. Salameh, and I. Khalil, "On the continuous coverage problem for a swarm of UAVs," in *Proc. IEEE 37th Sarnoff Symp.*, Newark, NJ, USA, Sep. 2016, pp. 130–135.
- [18] N. Kumar, M. Ghosh, and C. Singhal, "UAV network for surveillance of inaccessible regions with zero blind spots," in *Proc. IEEE INFOCOM Conf. Comput. Commun. Workshops (INFOCOM WKSHPs)*, Toronto, ON, Canada, Jul. 2020, pp. 1213–1218.
- [19] A. Bist and C. Singhal, "Efficient immersive surveillance of inaccessible regions using UAV network," in *Proc. IEEE INFOCOM Conf. Comput. Commun. Workshops (INFOCOM WKSHPs)*, May 2021, pp. 1–6.
- [20] A. Trotta, M. Di Felice, F. Montori, K. R. Chowdhury, and L. Bononi, "Joint coverage, connectivity, and charging strategies for distributed UAV networks," *IEEE Trans. Robot.*, vol. 34, no. 4, pp. 883–900, Aug. 2018.
- [21] J. Zhang, J. F. Campbell, D. C. Sweeney II, and A. C. Hupman, "Energy consumption models for delivery drones: A comparison and assessment," *Transp. Res. D, Transp. Environ.*, vol. 90, Jan. 2021, Art. no. 102668.
- [22] R. D'Andrea, "Guest editorial can drones deliver?" *IEEE Trans. Autom. Sci. Eng.*, vol. 11, no. 3, pp. 647–648, Jul. 2014.
- [23] K. Delmas, C. Seguin, and P. Bieber, "Tiered model-based safety assessment," in *Proc. Model-Based Saf. Assessment, Proc. Intern. Symp., (IMBSA)*, Berlin, Germany: Springer-Verlag, Oct. 2019, pp. 141–156.
- [24] M. N. Boukoberine, Z. Zhou, and M. Benbouzid, "A critical review on unmanned aerial vehicles power supply and energy management: Solutions, strategies, and prospects," *Appl. Energy*, vol. 255, Dec. 2019, Art. no. 113823.
- [25] S. Seng, G. Yang, X. Li, H. Ji, and C. Luo, "Energy-efficient communications in unmanned aerial relaying systems," *IEEE Trans. Netw. Sci. Eng.*, vol. 8, no. 4, pp. 2780–2791, Mar. 2021.
- [26] H. Zhou, F. Hu, M. Juras, A. B. Mehta, and Y. Deng, "Real-time video streaming and control of cellular-connected UAV system: Prototype and performance evaluation," *IEEE Wireless Commun. Lett.*, vol. 10, no. 8, pp. 1657–1661, Aug. 2021.
- [27] X. Chen, T. Tan, and G. Cao, "Energy-aware and context-aware video streaming on smartphones," in *Proc. IEEE 39th Int. Conf. Distrib. Comput. Syst. (ICDCS)*, Dallas, TX, USA, Jul. 2019, pp. 861–870.
- [28] T. Mekonnen, E. Harjula, A. Heikkinen, T. Koskela, and M. Ylianttila, "Energy efficient event driven video streaming surveillance using SleepyCAM," in *Proc. IEEE Int. Conf. Comput. Inf. Technol. (CIT)*, Helsinki, Finland, Aug. 2017, pp. 107–113.
- [29] J. Baek, S. Ik Han, and Y. Han, "Energy-efficient UAV routing for wireless sensor networks," *IEEE Trans. Veh. Technol.*, vol. 69, no. 2, pp. 1741–1750, Feb. 2020.
- [30] J. Peng, H. Gao, L. Liu, Y. Wu, and X. Xu, "FNTAR: A future network topology-aware routing protocol in UAV networks," in *Proc. IEEE Wireless Commun. Netw. Conf. (WCNC)*, May 2020, pp. 1–6.
- [31] Y. Xiao, Y. Cui, P. Savolainen, M. Siekkinen, A. Wang, L. Yang, A. Ylä-Jääski, and S. Tarkoma, "Modeling energy consumption of data transmission over Wi-Fi," *IEEE Trans. Mobile Comput.*, vol. 13, no. 8, pp. 1760–1773, Aug. 2014.
- [32] K. A. Magade and A. Patankar, "Techniques for load balancing in wireless LAN's," in *Proc. Int. Conf. Commun. Signal Process.*, Apr. 2014, pp. 1831–1836.
- [33] C. Singhal and K. Rahul, "LB-UAVnet: Load balancing algorithm for UAV based network using SDN," in *Proc. 22nd Int. Symp. Wireless Pers. Multimedia Commun. (WPMC)*, Nov. 2019, pp. 1–5.
- [34] L. K. Malviya and D. Tiwari, "LMP-DSR: Load balanced multi-path dynamic source routing protocol for mobile ad-hoc network," in *Proc. 4th Int. Conf. Comput., Commun. Netw. Technol. (ICCCNT)*, Tiruchengode, India, Jul. 2013, pp. 1–5.
- [35] C. Zhao, Q. Zeng, Y. Tang, and B. Yang, "Multi-path routing protocol for the video service in UAV-assisted VANETs," in *Proc. IEEE 94th Veh. Technol. Conf. (VTC-Fall)*, Norman, OK, USA, Sep. 2021, pp. 1–5.
- [36] M. Y. Arafat and S. Moh, "Routing protocols for unmanned aerial vehicle networks: A survey," *IEEE Access*, vol. 7, pp. 99694–99720, 2019.
- [37] C. Pu, "Jamming-resilient multipath routing protocol for flying ad hoc networks," *IEEE Access*, vol. 6, pp. 68472–68486, 2018.
- [38] C. Pu, "Link-quality and traffic-load aware routing for UAV ad hoc networks," in *Proc. IEEE 4th Int. Conf. Collaboration Internet Comput. (CIC)*, Philadelphia, PA, USA, Oct. 2018, pp. 71–79.
- [39] A. A. Deshpande, F. Chiariotti, and A. Zanella, "SMURF: Reliable multipath routing in flying ad-hoc networks," in *Proc. Medit. Commun. Comput. Netw. Conf. (MedComNet)*, Arona, Italy, Jun. 2020, pp. 1–8.
- [40] P. Xie, "An enhanced OLSR routing protocol based on node link expiration time and residual energy in ocean FANETS," in *Proc. 24th Asia-Pacific Conf. Commun. (APCC)*, Ningbo, China, Nov. 2018, pp. 598–603.
- [41] Z. Shaikh, S. Baidya, and M. Levorato, "Robust multi-path communications for UAVs in the urban IoT," in *Proc. IEEE Int. Conf. Sens., Commun. Netw. (SECON Workshops)*, Hong Kong, Jun. 2018, pp. 1–5.
- [42] S. R. Pokhrel, J. Jin, and H. L. Vu, "Mobility-aware multipath communication for unmanned aerial surveillance systems," *IEEE Trans. Veh. Technol.*, vol. 68, no. 6, pp. 6088–6098, Apr. 2019.
- [43] C. Pu, I. Ahmed, E. Allen, and K.-K. R. Choo, "A stochastic packet forwarding algorithm in flying ad hoc networks: Design, analysis, and evaluation," *IEEE Access*, vol. 9, pp. 162614–162632, 2021.
- [44] C. Pu, "Stochastic packet forwarding algorithm in flying ad hoc networks," in *Proc. IEEE Mil. Commun. Conf. (MILCOM)*, Norfolk, VA, USA, Nov. 2019, pp. 490–495.
- [45] X. Wang, X. Sun, W. Pan, T. Xu, and X. Li, "SRR: A lightweight routing protocol for opportunistic networks," in *Proc. IEEE 17th Int. Conf. Commun. Technol. (ICCT)*, Chengdu, China, Oct. 2017, pp. 588–592.
- [46] M. A. Lopez, M. Baddeley, W. T. Lunardi, A. Pandey, and J.-P. Giacalone, "Towards secure wireless mesh networks for UAV swarm connectivity: Current threats, research, and opportunities," in *Proc. 17th Int. Conf. Distrib. Comput. Sensor Syst. (DCOSS)*, Jul. 2021, pp. 319–326.
- [47] W. T. L. Teacy, J. Nie, S. McClean, and G. Parr, "Maintaining connectivity in UAV swarm sensing," in *Proc. IEEE Globecom Workshops*, Miami, FL, USA, Dec. 2010, pp. 1771–1776.
- [48] Y. Li, C. Tian, S. Diggavi, M. Chiang, and A. R. Calderbank, "Network resource allocation for competing multiple description transmissions," in *Proc. IEEE GLOBECOM Global Telecommun. Conf.*, Los Angeles, CA, USA, Dec. 2008, pp. 1493–1504.
- [49] M. M. Holland, R. G. Aures, and W. B. Heinzelman, "Experimental investigation of radio performance in wireless sensor networks," in *Proc. 2nd IEEE Workshop Wireless Mesh Netw.*, Reston, VA, USA, Sep. 2006, pp. 140–150.
- [50] M. Machedon-Pisu, "The impact of propagation media and radio interference on the performance of wireless sensor networks with MicaZ motes," in *Proc. Int. Conf. Optim. Electr. Electron. Equip. (OPTIM)*, Bran, Romania, May 2014, pp. 866–872.
- [51] I. Broustis and M. Paterakis, "On the feasibility of integrated MPEG teleconference and data transmission, over IEEE 802.11 w lans," in *Proc. Netw. Technol., Services, Protocols*, Athens, Greece, vol. 3042, May 2004, pp. 638–649.
- [52] D. Li and J. Pan, "Evaluating MPEG-4/AVC video streaming over IEEE 802.11 wireless distribution system," in *Proc. IEEE Wireless Commun. Netw. Conf.*, Las Vegas, NV, USA, Mar. 2008, pp. 2147–2152.

- [53] A. Huszak and S. Imre, "Analysing GOP structure and packet loss effects on error propagation in MPEG-4 video streams," in *Proc. 4th Int. Symp. Commun., Control Signal Process. (ISCCSP)*, Limassol, Cyprus, Mar. 2010, pp. 1–5.
- [54] A. O. Adeyemi-Ejeye, M. Alreshoodi, L. Al-Jobouri, M. Fleury, and J. Woods, "Packet loss visibility across SD, HD, 3D, and UHD video streams," *J. Vis. Commun. Image Represent.*, vol. 45, pp. 95–106, May 2017.
- [55] W. B. Heinzelman, A. P. Chandrakasan, and H. Balakrishnan, "An application-specific protocol architecture for wireless microsensor networks," *IEEE Trans. Wireless Commun.*, vol. 1, no. 4, pp. 660–670, Oct. 2002.



SUBHRAJIT BARICK received the B.Tech. degree in electronics and telecommunications engineering from the Biju Patnaik University of Technology (BPUT), India, in 2013, and the M.Tech. degree in communication engineering from the Indian Institute of Information Technology, Design and Manufacturing (IIITDM), India, in 2016. He is currently pursuing the Ph.D. degree with the Department of Electronics and Electrical Communication Engineering, IIT Kharagpur, India. His research interests include network resource management, UAV communication, and machine learning.

• • •



CHETNA SINGHAL (Senior Member, IEEE) received the B.Eng. degree in electronics and telecommunications from the University of Pune, India, in 2008, and the M.Tech. degree in computer technology and the Ph.D. degree from the Indian Institute of Technology (IIT) Delhi, in 2010 and 2015, respectively. She worked at the IBM Software Laboratory, New Delhi, as a Software Engineer, in 2010, for a year. She is currently a Visiting Researcher (an ERCIM Fellow) at the Department of Computer Science, RISE Research Institutes of Sweden. She has been an Assistant Professor with the Department of Electronics and Electrical Communication Engineering, IIT Kharagpur, since 2015. Her research interests include next generation heterogeneous wireless networks, with emphasis on cross-layer optimization, adaptive multimedia services, energy efficiency, and resource allocation.